Molecular Pharmacology Fast Forward. Published on November 18, 2004 as doi:10.1124/mol.104.006734

MOL 6734

Activation of the melastatin-related cation channel TRPM3 by D-erythro-sphingosine

Christian Grimm, Robert Kraft, Günter Schultz, Christian Harteneck

Institut für Pharmakologie, Charité Campus Benjamin Franklin, Thielallee 69-73, 14195 Berlin, Germany

Molecular Pharmacology Fast Forward. Published on November 18, 2004 as DOI: 10.1124/mol.104.006734
This article has not been copyedited and formatted. The final version may differ from this version.

Running title: Sphingosine activates TRPM3

Correspondence: Christian Harteneck

Institut für Pharmakologie

Charité Campus Benjamin Franklin,

Thielallee 69-73, 14195 Berlin, Germany

Tel.: +49-30-84451825, Fax: +49-30-84451818

Email: Christian.Harteneck@charite.de

Text pages: 29
Figures: 6
Tables: 0
References: 37
Number of words in the abstract: 152
Number of words in the introduction: 477
Number of words in the discussion: 1111

Abbreviations: BIM I, 2-[1-(3-Dimethylaminopropyl)-1H-indol-3-yl]-3-(1H-indol-3-yl)-maleimide; C2-Cer, N-acetyl-D-erythro-sphingosine; C8-Cer, N-octanoyl-D-erythro-sphingosine; DDG, 1,2-didecanoyl-rac-glycerol; DHS, dihydro-D-erythro-sphingosine; DMS, N,N-dimethyl-D-erythro-sphingosine; Gö 6976, 12-(2-Cyanoethyl)-6,7,12,13-tetrahydro-13-methyl-5-oxo-5H-indolo(2,3-a)pyrrolo(3,4-c)-carbazole; OAG, 1-oleoyl-2-acetyl-sn-glycerol; SOCE, store operated calcium entry; S1P, D-erythro-sphingosine-1-phosphate; TRP, transient receptor potential; YFP, yellow fluorescent protein

Molecular Pharmacology Fast Forward. Published on November 18, 2004 as DOI: 10.1124/mol.104.006734
This article has not been copyedited and formatted. The final version may differ from this version.

Abstract

TRPM3, a member of the melastatin-like transient receptor potential channel subfamily (TRPM), is predominantly expressed in human kidney and brain. TRPM3 mediates spontaneous Ca^{2+} entry and nonselective cation currents in transiently transfected HEK293 cells. Using measurements with the Ca^{2+}-sensitive fluorescent dye fura-2 and the whole-cell patch clamp technique, we found that D-erythro-sphingosine, a metabolite arising during the de novo synthesis of cellular sphingolipids, activated TRPM3. Other TRP channels tested (TRPC3, TRPC4, TRPC5, TRPV4, TRPV5, TRPV6 and TRPM2) did not significantly respond to application of sphingosine. Sphingosine-induced TRPM3 activation was not mediated by inhibition of protein kinase C, depletion of intracellular Ca^{2+} stores and intracellular conversion of sphingosine to sphingosine-1-phosphate. While sphingosine-1-phosphate and ceramides had no effect, two structural analogues of sphingosine, dihydro-D-erythro-sphingosine and N,N-dimethyl-D-erythro-sphingosine, also activated TRPM3. Sphingolipids, including sphingosine, are known to have inhibitory effects on a variety of ion channels. Thus, TRPM3 is the first ion channel activated by sphingolipids.

Molecular Pharmacology Fast Forward. Published on November 18, 2004 as DOI: 10.1124/mol.104.006734
This article has not been copyedited and formatted. The final version may differ from this version.

Introduction

Transient receptor potential (TRP) proteins form a superfamily of non-selective cation channels containing six putative transmembrane domains, with the pore forming region between the fifth and sixth segment, and cytosolic C and N termini (Clapham, 2003). Three main subfamilies of TRP channels have been described: TRPC (C for ”classical” or ”canonical”), TRPV (V for ”vanilloid receptor-like”) and TRPM (M for ”melastatin-like”) (Montell et al., 2002a). TRP members are expressed in a variety of organisms and cell types and are activated by various signals from both inside and outside the cell, such as hormones, temperature, cell swelling, Ca^{2+}, and endogenous or synthetic ligands (Montell et al., 2002b; Clapham, 2003). Thereby, ligand-mediated regulation is the most frequently observed activation mechanism within the TRP superfamily. Arachidonic acid (AA) and linolenic acid were shown to activate *Drosophila* TRP and TRPL channels (Chyb et al., 1999). Other lipid mediators, such as diacylglycerol analogues, were described to open the mammalian TRPC channels TRPC3, TRPC6 and TRPC7 (Hofmann et al., 1999; Okada et al., 1999). TRPV1 and the related channel TRPV4 have been shown to be opened by the endocannabinoid anandamide and its metabolite arachidonic acid (Zygmunt et al., 1999; Watanabe et al., 2003). Products of the lipoxygenase and P450 epoxygenase pathways of the arachidonic acid metabolism were identified as potent activators of TRPV1 and TRPV4, respectively (Hwang et al., 2000; Watanabe et al., 2003).

We have recently characterized a TRPM3 variant containing 1325 aa as a spontaneously active, Ca^{2+}-permeable cation channel, which is stimulated by hypotonic cell swelling (Grimm et al., 2003). This TRPM3 variant was cloned from human fetal brain, and its native expression in human brain and kidney was confirmed by Western blot analysis using a specific TRPM3 antibody (Grimm et al., 2003). The swelling-induced activation of another TRP channel, TRPV4, has been shown to be

Molecular Pharmacology Fast Forward. Published on November 18, 2004 as DOI: 10.1124/mol.104.006734
This article has not been copyedited and formatted. The final version may differ from this version.

based on the formation of arachidonic acid (AA) and its derivative 5‘,6‘-epoxyeicosatrienoic acid (5‘,6‘-EET) (Vriens et al., 2003). While fatty acids or lipid metabolites from the phospholipase C (PLC) and phospholipase A_2 (PLA_2) pathway were ineffective as activators of TRPM3, we found an activation of TRPM3 by the sphingolipid D-erythro-sphingosine (SPH) and by SPH analogues. SPH is a central metabolite arising during the de novo synthesis of cellular sphingolipids. The equilibrium of ceramides, SPH, and D-erythro-sphingosine-1-phosphate (S1P) plays a key role in regulating growth, differentiation, survival and cell death (Huwiler et al., 2000). Members of the melastatin subfamily of TRP channels are apparently involved in cell death and regulation of cell proliferation (Duncan et al., 1998; Hara et al., 2002; Aarts et al., 2003; Hanano et al., 2004). In contrast to SPH, neither ceramides nor S1P, AA, or diacylglycerol analogues were able to stimulate TRPM3. We show here for the first time that an ion channel, TRPM3, is activated by SPH and may be involved in SPH-induced Ca^{2+} entry in a multiplicity of cellular systems.

Molecular Pharmacology Fast Forward. Published on November 18, 2004 as DOI: 10.1124/mol.104.006734
This article has not been copyedited and formatted. The final version may differ from this version.

Materials and Methods

Cell culture and transfections

HEK293 cells were cultured in Earle´s MEM (Biochrom, Berlin, Germany), supplemented with 10 % FCS (Biochrom), 100 µg/ml penicillin, 100 µg/ml streptomycin under 5 % CO_2 atmosphere at 37°C. Cells were plated in 85 mm dishes onto glass coverslips and transiently transfected with 1.5 - 2 µg of DNA and 5 µl of FuGENE 6 transfection reagent (Roche, Indianapolis, IN, USA) in 95 µl of OptiMEM medium vector (Invitrogen, Groningen, The Netherlands) 48 h later. The cDNAs of the following TRP channels C-terminally fused to enhanced green (eGFP) or yellow (YFP) fluorescent proteins were used: hsTRPC3 (GenBank number NM003305), mmTRPC4 (GenBank number NM016984), mmTRPC5 (GenBank number NM009428), hsTRPV4 (GenBank number NM147204), mmTRPV5 (GenBank number XM112633), mmTRPV6 (GenBank number NM022413), hsTRPM2 (GenBank number NM003307) and hsTRPM3 (GenBank number AJ505026).

Fluorescence measurements

Measurements of intracellular Ca^{2+} concentration ($[Ca^{2+}]_i$) in single cells were carried out using the fluorescent indicator fura-2 in combination with a monochromator-based imaging system (T.I.L.L. Photonics, Gräfelfing, Germany) attached to an inverted microscope (Axiovert 100, Zeiss, Oberkochen, Germany). HEK293 cells were loaded with 4 µM fura-2-AM (Molecular Probes, Leiden, The Netherlands) in a standard solution as previously described (Grimm et al., 2003). Osmolarity effects were studied in a solution with 88 instead of 138 mM NaCl, containing 0 and 100 mM mannitol, resulting in osmolarities of 200 and 300 mosmol/l, respectively. Fluorescence

Molecular Pharmacology Fast Forward. Published on November 18, 2004 as DOI: 10.1124/mol.104.006734
This article has not been copyedited and formatted. The final version may differ from this version.

quenching by Mn^{2+} entry and $[Ca^{2+}]_i$ measurements were carried out as previously described (Grimm et al., 2003).

Patch clamp measurements

Membrane currents were recorded in the whole-cell configuration of the patch-clamp technique, using an Axopatch 200 B amplifier (Axon Instruments, CA, USA), subsequently low-pass filtered at 1 kHz, digitized with a sampling rate of 5 kHz and analyzed, using pCLAMP software (version 7.0; Axon Instruments). The pipette resistance varied between 3 - 5 MΩ. Pipettes were filled with a solution composed of 130 mM $CsCH_3O_3S$, 10 mM CsCl, 5 mM $MgCl_2$, 10 mM HEPES and 10 mM 1,2-bis(2-aminophenoxy)ethane-N,N,N´,N´-tetraacetic acid (BAPTA) (pH 7.2 with CsOH). The bath solution contained 140 mM NaCl, 2 mM $CaCl_2$, 1 mM $MgCl_2$, 10 mM glucose and 10 mM HEPES (pH 7.4 with NaOH). For Na^+-free conditions, Na^+ was replaced with 140 mM N-methyl-D-glucamine ($NMDG^+$). In some experiments, extracellular solution contained 100 mM $CaCl_2$. Whole-cell currents were elicited by either voltage ramps (400 msec duration) applied every 5 sec from a holding potential of 0 mV or by voltage steps as shown in Figure 4. Voltage ramps were elicited from either -100 mV to +100 mV or +100 mV to –100 mV. Relative cation permeabilities were calculated as described previously (Grimm et al., 2003). All pooled data from patch-clamp experiments are expressed as means ± SEM from n cells.

Chemicals

D-erythro-sphingosine (SPH), dihydro-D-erythro-sphingosine (DHS), N,N-dimethyl-D-erythro-sphingosine (DMS), N-acetyl-D-erythro-sphingosine (C2-Cer) and N-octanoyl-D-erythro-sphingosine (C8-Cer) (Calbiochem) were diluted from 20 mM stock solutions in ethanol, D-erythro-sphingosine-1-phosphate (S1P) (Calbiochem) from a

Molecular Pharmacology Fast Forward. Published on November 18, 2004 as DOI: 10.1124/mol.104.006734
This article has not been copyedited and formatted. The final version may differ from this version.

10 mM stock solution in methanol, arachidonic acid (AA) and anandamide (AEA) (Sigma) from 50 mM stock solutions in ethanol, linolenic acid (LNA) and linoleic acid (LA), (Sigma) from 100 mM stock solutions in ethanol, 1-oleoyl-2-acetyl-sn-glycerol (OAG) and 1,2-didecanoyl-rac-glycerol (DDG) (Calbiochem) from 100 mM stock solutions in DMSO.

Molecular Pharmacology Fast Forward. Published on November 18, 2004 as DOI: 10.1124/mol.104.006734
This article has not been copyedited and formatted. The final version may differ from this version.

Results

Activation of TRPM3 by SPH

Extracellular application of SPH (20 μM) induced an increase in $[Ca^{2+}]_i$ in TRPM3-transfected HEK293 cells within 20 - 30 s after start of application, whereas non-transfected control cells (NT) showed only very small responses (Fig. 1A). Exchange of extracellular Ca^{2+} for EGTA (2 mM) almost completely inhibited these $[Ca^{2+}]_i$ increases, indicating Ca^{2+} influx via the plasma membrane (Fig. 1A). In the presence of EGTA and before adding extracellular Ca^{2+}, SPH induced no effects in TRPM3-transfected HEK293 cells (Fig. 1B). In fura-2 quench experiments using 200 μM Mn^{2+}, the spontaneous activity of TRPM3-transfected HEK293 cells was enhanced after application of 20 μM SPH, whereas non-transfected control cells showed only weak effects (Fig. 1C). The concentration of SPH for half-maximal activation of TRPM3 was 12 μM obtained from increases in $[Ca^{2+}]_i$ (Fig. 1D). Application of SPH (20 μM) as well as application of hypotonic extracellular solution each produced increases in $[Ca^{2+}]_i$ with comparable amplitudes in individual cells (Fig. 1E). Peak values of SPH-induced increases in $[Ca^{2+}]_i$ in TRPM3-transfected cells were not exceeded by additional application of hypotonic extracellular solution (200 mosmol/l) (Fig. 1F). This suggests that treatment with 20 μM SPH and hypotonic stimulation are not additive.

Specificity of the TRPM3 activation by SPH

In contrast to TRPM3, other members of the TRP family transiently transfected in HEK293 cells (hsTRPC3, mmTRPC4, mmTRPC5, hsTRPV4, mmTRPV5, mmTRPV6, hsTRPM2) were not significantly activated by SPH compared to non-transfected control cells (Fig. 2A). Diverse TRP channels are activated by fatty acids

Molecular Pharmacology Fast Forward. Published on November 18, 2004 as DOI: 10.1124/mol.104.006734
This article has not been copyedited and formatted. The final version may differ from this version.

or lipids, particularly by products of the phospholipase C and phospholipase A_2 pathway (Chyb et al., 1999, Hofmann et al., 1999; Okada et al., 1999). We therefore examined a possible activation of TRPM3 by such substances. However, no significant differences were detectable in TRPM3-transfected cells compared to nontransfected control cells upon application (100 μM each) of anandamide (AEA), arachidonic acid (AA), linolenic acid (LNA), linoleic acid (LA), 1-oleoyl-2-acetyl-sn-glycerol (OAG) or 1,2-didecanoyl-rac-glycerol (DDG) (Fig. 2B). A TRP channel distantly related to TRPM3, TRPC3, has been described to be activated by diacylglycerol analogues (Hofmann et al., 1999). In parallel fura-2 experiments the effects of the diacylglycerol analogue DDG and SPH were tested in HEK293 cells transiently transfected with either TRPC3 or TRPM3 (Fig. 2C). While TRPC3-expressing cells clearly responded to application of 100 μM DDG, 20 μM SPH did not significantly increase $[Ca^{2+}]_i$ in these cells (Fig. 2D). On the other hand, in TRPM3-expressing cells the $[Ca^{2+}]_i$ was not significantly elevated by application of 100 μM DDG. Instead, 20 μM SPH increased $[Ca^{2+}]_i$ in TRPM3-expressing cells (Fig. 2E).

SPH-induced currents through TRPM3

In TRPM3-transfected cells, extracellular SPH (10 μM) induced whole-cell currents which could be resolved on the single-channel level during the onset of activation within a time period of about 30 s after start of application (Fig. 3A). At a holding potential of -60 mV, single channel openings with an amplitude of about -4.5 pA (n = 3) were detected, corresponding to a chord conductance of 75 pS. From the current-voltage relationship of the SPH-induced single channel currents, we calculated a slope conductance of 73 pS for inward currents (Fig. 3B). Current-voltage relationships of SPH-induced whole-cell currents during voltage-ramps (starting from

Molecular Pharmacology Fast Forward. Published on November 18, 2004 as DOI: 10.1124/mol.104.006734
This article has not been copyedited and formatted. The final version may differ from this version.

negative potentials) showed a clear outward rectification (Fig. 3C). Exchange of extracellular Na^+-containing solution for 100 mM $CaCl_2$ induced a rapid and transient increase in SPH-induced inward currents and a shift of the reversal potential toward more positive voltages (Fig. 3C). Application of a solution containing $NMDG^+$ suppressed these inward currents, indicating permeation of Ca^{2+} through TRPM3 channels (Fig. 3C). Figure 3D shows the voltage dependence of the current densities under different ionic conditions. In the presence of Na^+-containing bath solution, the mean currents were –9.3 ± 2.4 pA/pF and 33.3 ± 5.8 pA/pF (n = 10) at –100 mV and +100 mV, respectively. In the presence of 100 mM $CaCl_2$, current densities were -59.3 ± 7.2 pA/pF and 47.2 ± 5.6 pA/pF (n = 10), respectively. To explore a possible voltage modulation of TRPM3, we applied 500 ms voltage steps from a holding potential of 0 mV. During application of SPH on TRPM3-transfected cells, currents showed a time-dependent increase during prolonged depolarization and a decrease during hyperpolarization (Fig. 4A). Current-voltage relationships observed during different test potentials after a prestep to +100 mV revealed a linear voltage dependence of instantaneous currents (Fig. 4B), similarly to the instantaneous currents through the voltage-dependent channels TRPM4 and TRPM8 (Nilius et al., 2003; Voets et al., 2004). However, in contrast to currents through TRPM4 and TRPM8, we did not find a complete deactivation of TRPM3-mediated inward currents at negative test potentials and holding potentials of 0 mV (Fig. 4B) or –90 mV (data not shown). To investigate a possible voltage dependence of TRPM3 open probability, we measured the current amplitude during a voltage step to –100 mV following different presteps (Fig. 4C). The fraction of open channels (F_{open}) at the end of each prestep potential was calculated by normalizing the current amplitudes at the beginning of the step to -100 mV to their maximal value. The resulting F_{open}-voltage relationships could be fitted by a Boltzmann function (Fig. 4C), as described

Molecular Pharmacology Fast Forward. Published on November 18, 2004 as DOI: 10.1124/mol.104.006734
This article has not been copyedited and formatted. The final version may differ from this version.

previously (Nilius et al., 2004). The mean slope of these fits, obtained from individual TRPM3-transfected cells treated with 10 µM SPH, was 22.3 ± 1.7 mV (n = 6). The voltage for half-maximal activation varied from cell to cell and ranged from –67 mV to +113 mV. To investigate the relative cation permeability of SPH-activated TRPM3 channels we applied voltage ramps from +100 to –100 mV following 500 ms long prepulses to +100 mV. Under these conditions, a hyperpolarization-induced deactivation of TRPM3 should be attenuated. Indeed, upon application of SPH the current activation was much steeper (Fig. 4D) than in continuous recordings at –60 mV (Fig. 3A) or in conventional voltage ramp recordings (Fig. 3C). Exchange of Na^+-containing solution for 100 mM $CaCl_2$ shifted the reversal potentials of the current-voltage relationships from +1.2 ± 2.0 mV (n = 5) to +10.2 ± 4.4 mV (n = 5) (Fig. 4D). Application of 140 mM NMDG-Cl nearly completely abolished inward currents, suggesting permeation through a cation channel. From the shifts of the reversal potentials during subsequent application of Na^+ and Ca^{2+}, a relative permeability P_{Ca}/P_{Na} = 1.91 ± 0.51 (n = 5) was calculated. The ion concentrations were corrected for the respective activity coefficients (0.76 for 140 mM NaCl, 0.517 for 100 mM $CaCl_2$).

Effects of SPH after store depletion, inhibition of inositol 1,4,5-trisphosphate (IP_3) receptors or inhibition of PKC

To test whether TRPM3 activation by SPH is independent of Ca^{2+} store depletion, we used thapsigargin (5 µM), an inhibitor of smooth endoplasmic reticulum Ca^{2+}-ATPase, which induces store-operated Ca^{2+} entry. SPH, described to inhibit calcium release-activated calcium current (I_{CRAC}) in RBL-2H3 cells (Mathes et al., 1998), blocked the thapsigargin-evoked Ca^{2+} signals in non-transfected HEK293 cells (Fig. 5A), whereas

Molecular Pharmacology Fast Forward. Published on November 18, 2004 as DOI: 10.1124/mol.104.006734
This article has not been copyedited and formatted. The final version may differ from this version.

it induced $[Ca^{2+}]_i$ increases in TRPM3-transfected cells (Fig. 5B). To exclude a possible involvement of inositol 1,4,5-trisphosphate (IP_3) receptors in SPH-mediated activation of TRPM3, we applied the IP_3 receptor inhibitor xestospongin C (1 μM). However, responses to SPH were not influenced by pretreatment with xestospongin C (Fig. 5C). SPH has originally been described as an inhibitor of protein kinase C (PKC) (Smith et al., 2000). Application of several known PKC inhibitors, i.e. BIM I (1 μM, Fig. 5D), calphostin C or Gö 6976 (1 μM each, data not shown), and of an inhibitor of protein kinases, staurosporine (1 μM, Fig. 5D), did not induce significant changes in $[Ca^{2+}]_i$ in TRPM3-transfected cells compared to non-transfected cells.

Effects of other sphingolipids

We tested sphingolipids from the sphingomyelin pathway that are structurally related to SPH (Fig. 6A). Dihydro-D-erythro-sphingosine (DHS) and N,N-dimethyl-D-erythro-sphingosine (DMS) also induced increases in $[Ca^{2+}]_i$ (Fig. 6B). No significant effects were measured after external application of the membrane-permeable ceramides N-acetyl-D-erythro-sphingosine (C2-Cer, 20 μM) and N-octanoyl-D-erythro-sphingosine (C8-Cer, 20 μM), and of S1P (10 μM) (Fig. 6C). Extracellularly applied S1P produced a similar increase in $[Ca^{2+}]_i$ both in TRPM3-transfected and non-transfected cells, probably due to an activation of G-protein-coupled S1P receptors which are endogenously expressed in HEK293 cells (Meyer zu Heringdorf et al., 2001). To test for a possible S1P-mediated activation of TRPM3 from the intracellular side, we perfused TRPM3-transfected cells with S1P (10 μM) via the patch pipette. During a time interval of at least 2 min after attaining the whole-cell configuration, no steady increase in currents could be observed (n = 4; Fig. 6D). Subsequent application of SPH (10 μM) via the bath solution induced currents with similar properties to those

Molecular Pharmacology Fast Forward. Published on November 18, 2004 as DOI: 10.1124/mol.104.006734
This article has not been copyedited and formatted. The final version may differ from this version.

shown in Figure 4D. To further exclude an activation of TRPM3 through intracellular conversion of SPH to S1P, we used DMS which is also known as an inhibitor of sphingosine kinases which specifically phosphorylate SPH to S1P (Edsall et al., 1998; Huwiler et al., 2000). However, pretreatment with DMS (10 µM, data not shown) was not able to reduce SPH evoked increases in $[Ca^{2+}]_i$ in TRPM3-transfected HEK293 cells, indicating that SPHK activity and phosphorylation of SPH to S1P are not required for TRPM3 activation.

Molecular Pharmacology Fast Forward. Published on November 18, 2004 as DOI: 10.1124/mol.104.006734
This article has not been copyedited and formatted. The final version may differ from this version.

Discussion

The present study shows that a previously described TRPM3 variant containing 1325 aa (Grimm et al., 2003) is activated by SPH, independently of PKC inhibition, formation of S1P or intracellular Ca^{2+} store depletion.

Electrophysiological investigation of this TRPM3 variant yielded a single channel conductance for SPH-induced currents of about 75 pS. This is in accordance with the previously reported value of 83 pS for spontaneously active TRPM3 channels in the presence of extracellular Na^+ (Grimm et al., 2003). From whole-cell currents in the presence of either extracellular Na^+ or Ca^{2+}, a relative permeability P_{Ca}/P_{Na} = 1.91 was calculated. This value is close to the relative permeability P_{Ca}/P_{Na} = 1.57 determined for spontaneously active TRPM3 channels (Grimm et al., 2003). In the presence of 100 mM extracellular Ca^{2+}, the outward rectification of SPH-induced currents appears to be replaced by an inward and outward rectification, resulting in a S-like current-voltage relationship (see Fig. 3D). SPH-induced currents elicited by voltage steps were characterized by an activation at positive potentials and a deactivation at negative potentials. This resembles the kinetic behaviour of some other TRPM channels, i.e. TRPM4, TRPM5 and TRPM8 (Nilius et al., 2003; Hofmann et al., 2003; Voets et al., 2004). From fits to the Boltzman function, giving a value of about 22 mV for an e-fold increase in open probability, we suggest a voltage dependence of TRPM3 channels. The voltage for half-maximal activation of TRPM3 channels in the presence of 10 µM SPH, however, was quite different between individual cells ranging from –67 mV to +113 mV. Therefore, the definition of a SPH-induced shift of the activation curve at appropriate membrane potentials, as shown for the menthol- and temperature-dependent activation of TRPM8 (Voets et al., 2004), was not possible. The variable voltages for half-maximal activation of TRPM3 may be due to differences in the distribution and binding of the lipid compound SPH to the channels in individual

Molecular Pharmacology Fast Forward. Published on November 18, 2004 as DOI: 10.1124/mol.104.006734
This article has not been copyedited and formatted. The final version may differ from this version.

cells. Furthermore, the concentration of endogeneous SPH inducing spontaneous activity of TRPM3, may vary from cell to cell.

Hofmann *et al.* (1999) reported that the intracellular release of diacylglycerols after activation of G-protein coupled receptors and PLC induces opening of TRPC3 and TRPC6 channels. In this approach, the rate of Mn^{2+} entry following extracellular application of DAG analogues was slower than after receptor stimulation (Hofmann et al., 1999). This slower activation kinetics could be explained by a delay due to incorporation and accumulation of DAG analogues in the plasma membrane and/or the cytosol. In analogy, the long latency for activation of TRPM3 could also be due to an action of SPH in a membrane-delimited manner or from the intracellular face of the channel. This was substantiated by Ca^{2+} imaging experiments, in which activation of TRPC3 by the DAG analogue DDG showed the same kinetics as those for TRPM3 by SPH (see Fig. 2D and 2E).

Lee *et al.* (2003) have recently described six TRPM3 splice variants named TRPM3a - TRPM3f. Due to a shorter N-terminus (153 aa) and a longer C-terminus (382 aa) compared with our variant (Grimm et al., 2003), these proteins consist of 1545 to 1580 amino acids. TRPM3a - TRPM3f differ by small deletions and insertions (12-25 aa) in the N-terminus or the pore forming domain. One variant, TRPM3a, has been shown to mediate spontaneous Ca^{2+} entry after transfection in HEK293 cells (Lee et al., 2003). The different C-terminal ends of the TRPM3 variants described by Lee *et al.* (2003) and of our TRPM3 variant have been independently confirmed by mouse EST clones. EST accession AK173218 corresponds to the C-terminal ends of TRPM3a – TRPM3f (Lee et al., 2003) and EST accession AK051867 corresponds to the C-terminus of our variant (Grimm et al., 2003). Whether this differential splicing may result in different activation mechanisms and physiological functions has still to be elucidated.

Molecular Pharmacology Fast Forward. Published on November 18, 2004 as DOI: 10.1124/mol.104.006734
This article has not been copyedited and formatted. The final version may differ from this version.

The involvement of TRP channels in the sphingolipid pathway has not been investigated to date, and TRPM3 is the first TRP superfamily member described to be activated by SPH and SPH analogues. We show here that a variety of other TRP channels of all three subfamilies are not significantly activated by SPH. Sphingolipids, in particular SPH, have been described to inhibit ion channels, such as voltage-gated Ca^{2+} channels (McDonough et al., 1994; Titievsky et al., 1998), the skeletal muscle ryanodine receptor (Needleman et al., 1997; Sharma et al., 2000), and channels mediating I_{CRAC} in RBL-2H3 cells (Mathes et al., 1998). The activation of an ion channel by SPH has not been shown so far.

Although structural analogues to SPH, e.g. DHS and DMS, activated TRPM3, ceramides and S1P had no effect. S1P is the ligand for a family of five G-protein-coupled receptors ($S1P_1$ - $S1P_5$). They are ubiquitously expressed, couple to various G-proteins and regulate e.g. angiogenesis, vascular maturation and cardiac development (Spiegel et al., 2003). Intracellularly, S1P generated from SPH through phosphorylation by sphingosine kinases (SPHK) (Huwiler et al., 2000; Maceyka et al., 2002) plays a role as a second messenger with Ca^{2+} release activity (Gosh et al., 1990; Young et al., 2002). In patch-clamp and calcium imaging experiments we show that both intracellular and extracellular application of S1P does not activate TRPM3. We therefore conclude that activation of TRPM3 by SPH is independent of the phosphorylation of SPH to S1P.

The activation of the sphingomyelinase/ceramidase pathway, e.g. by growth factors (Jacobs et al., 1993; Coroneos et al., 1995) or by cell swelling, may result in prolonged Ca^{2+} entry in cells endogenously expressing TRPM3. Activation of TRPV4 is reported to be based on swelling-induced activation of phospholipase A_2 and cytochrome P450 epoxygenase (Vriens et al., 2004). Cell swelling and hypotonic stress can also activate tyrosine kinases in cardiac myocytes (Sadoshima et al.,

1996) and the receptor-tyrosine-kinase EGFR in fibroblasts (Franco et al., 2004). Thus, cell swelling may induce activation of TRPM3 directly or indirectly by activation of the sphingomyelinase/ceramidase pathway resulting in release and intracellular accumulation of SPH as breakdown product of sphingomyelin/ceramides whereby sphingomyelin accounts for approximately 10 to 15% of total cellular phospholipid content (Zager et al., 2000).

Finally, our data do not support any contribution of Ca^{2+} store depletion to the activation of TRPM3. The endogenous store-operated Ca^{2+} entry in non-transfected HEK293 cells was blocked by SPH which is in agreement with the inhibitory action of SPH on I_{CRAC} in RBL-2H3 cells (Mathes et al., 1998). Depletion of intracellular Ca^{2+} stores induced by the activation of PLC through the release of IP_3 and the opening of endoplasmic IP_3 receptors has been confirmed in a large number of cell types. Formation of SPH, e.g. by activation of receptor tyrosine kinases, thus results in an inhibition of store-operated Ca^{2+} entry while a compensatory Ca^{2+} influx may occur in TRPM3-expressing cells.

Molecular Pharmacology Fast Forward. Published on November 18, 2004 as DOI: 10.1124/mol.104.006734
This article has not been copyedited and formatted. The final version may differ from this version.

Acknowledgements

We thank Inge Reinsch for technical assistance, Tim Plant for critical reading of the manuscript and Michael Schaefer for providing the TRPC4 and TRPC5 cDNAs.

References

Aarts M, Iihara K, Wie WL, Xiong ZG, Arundine M, Cerwinski W, MacDonald JF, and Tymianski M (2003) A key role for TRPM7 channels in anoxic neuronal death. *Cell* **115:**863-877.

Chyb S, Raghu P, and Hardie RC (1999) Polyunsaturated fatty acids activate the Drosophila light-sensitive channels TRP and TRPL. *Nature* **397:**255-259.

Clapham DE (2003) TRP channels as cellular sensors. *Nature* **426:**517-524.

Coroneos E, Martinez M, McKenna S, and Kester M (1995) Differential regulation of sphingomyelinase and ceramidase activities by growth factors and cytokines. Implications for cellular proliferation and differentiation. *J Biol Chem* **270:**23305-23309.

Duncan LM, Deeds J, Hunter J, Shao J, Holmgren LM, Woolf EA, Tepper RI, and Shyjan AW (1998) Down-regulation of the novel gene melastatin correlates with potential for melanoma metastasis. *Cancer Res* **58:**1515-1520.

Grimm C, Kraft R, Sauerbruch S, Schultz G, and Harteneck, C (2003) Molecular and functional characterization of the melastatin-related cation channel TRPM3. *J Biol Chem* **278:**21493-21501.

Edsall LC, Van Brocklyn JR, Cuvillier O, Kleuser B, and Spiegel S (1998) N,N-Dimethylsphingosine is a potent competitive inhibitor of sphingosine kinase but not of protein kinase C: modulation of cellular levels of sphingosine 1-phosphate and ceramide. *Biochemistry* **37:**12892-12898.

Franco R, Lezama R, Ordaz B, and Pasantes-Morales H (2004) Epidermal growth factor receptor is activated by hyposmolarity and is an early signal modulating osmolyte efflux pathways in Swiss 3T3 fibroblasts. *Pflügers Arch* **447:**830-839.

Ghosh TK, Bian J, and Gill DL (1990) Intracellular calcium release mediated by sphingosine derivatives generated in cells. *Science* **248:**1653-1656.

Hanano T, Hara Y, Shi J, Morita H, Umebayashi C, Mori E, Sumimoto H, Ito Y, Mori Y, and Inoue R (2004) Involvement of TRPM7 in cell growth as a spontaneously activated Ca^{2+} entry pathway in human retinoblastoma cells. *J Pharmacol Sci* **95:**403-419.

Hara Y, Wakamori M, Ishii M, Maeno E, Nishida M, Yoshida T, Yamada H, Shimizu S, Mori E, Kudoh J, Shimizu N, Kurose H, Okada Y, Imoto K, and Mori Y (2002) LTRPC2 Ca^{2+}-permeable channel activated by changes in redox status confers susceptibility to cell death. *Mol Cell* **9:**163-173.

Hofmann T, Obukhov AG, Schaefer M, Harteneck C, Gudermann T, and Schultz G (1999). Direct activation of human TRPC6 and TRPC3 channels by diacylglycerol. *Nature* **397:**259-263.

Hofmann T, Chubanov V, Gudermann T, and Montell C (2003) TRPM5 is a voltage-modulated and Ca^{2+}-activated monovalent selective cation channel. *Curr Biol* **13:**1153-1158.

Huwiler A, Kolter T, Pfeilschifter J, and Sandhoff K (2000) Physiology and pathophysiology of sphingolipid metabolism and signaling. *Biochim Biophys Acta* **1485:**63-99.

Hwang SW, Cho H, Kwak J, Lee SY, Kang CJ, Jung J, Cho S, Min KH, Suh YG, Kim D, and Oh U (2000) Direct activation of capsaicin receptors by products of lipoxygenases: endogenous capsaicin-like substances. *Proc Natl Acad Sci USA* **97:**6155-6160.

Jacobs LS and Kester M (1993) Sphingolipids as mediators of effects of platelet-derived growth factor in vascular smooth muscle cells. *Am J Physiol* **265:**C740-747.

Lee N, Chen J, Sun L, Wu S, Gray KR, Rich A, Huang M, Lin JH, Feder JN, Janovitz EB, Levesque PC, and Blanar, MA (2003) Expression and characterization of human transient receptor potential melastatin 3 (hTRPM3). *J Biol Chem* **278:**20890-20897.

Maceyka M, Payne SG, Milstien S, and Spiegel S (2002) Sphingosine kinase, sphingosine-1-phosphate, and apoptosis. *Biochim Biophys Acta* **1585:**193-201.

Mathes C, Fleig A, and Penner R (1998) Calcium release-activated calcium current (I_{CRAC}) is a direct target for sphingosine. *J Biol Chem* **273:**25020-25030.

McDonough PM, Yasui K, Betto R, Salviati G, Glembotski CC, Palade PT, and Sabbadini RA (1994) Control of cardiac Ca^{2+} levels. Inhibitory actions of sphingosine on Ca^{2+} transients and L-type Ca^{2+} channel conductance. *Circ Res* **75:**981-989.

Meyer zu Heringdorf D, Lass H, Kuchar I, Lipinski M, Alemany R, Rumenapp U, and Jakobs KH (2001) Stimulation of intracellular sphingosine-1-phosphate production by G-protein-coupled sphingosine-1-phosphate receptors. *Eur J Pharmacol* **414:**145-154.

Montell C, Birnbaumer L, Flockerzi V, Bindels RJ, Bruford EA, Caterina MJ, Clapham DE, Harteneck C, Heller S, Julius D, Kojima I, Mori Y, Penner R, Prawitt D, Scharenberg, AM Schultz, G, Shimizu N, and Zhu MX (2002a) A unified nomenclature for the superfamily of TRP cation channels. *Mol Cell* **9:**229-231.

Montell C, Birnbaumer L, and Flockerzi V (2002b) The TRP channels, a remarkably functional family. *Cell* **108:**595-598.

Needleman DH, Aghdasi B, Seryshev AB, Schroepfer GJ Jr, and Hamilton SL (1997) Modulation of skeletal muscle Ca^{2+}-release channel activity by sphingosine. *Am J Physiol* **272:**C1465-1474.

Nilius B, Prenen J, Droogmans G, Voets T, Vennekens R, Freichel M, Wissenbach U, and Flockerzi V (2003) Voltage dependence of the Ca^{2+}-activated cation channel TRPM4. *J Biol Chem* **278:**30813-30820.

Okada T, Inoue R, Yamazaki K, Maeda A, Kurosaki T, Yamakuni T, Tanaka I, Shimizu S, Ikenaka K, Imoto K, and Mori Y (1999) Molecular and functional characterization of a novel mouse transient receptor potential protein homologue TRP7 Ca^{2+}-permeable cation channel that is constitutively activated and enhanced by stimulation of G protein-coupled receptor. *J Biol Chem* **274:**27359-27370.

Sadoshima J, Qiu Z, Morgan JP, and Izumo S (1996) Tyrosine kinase activation is an immediate and essential step in hypotonic cell swelling-induced ERK activation and c-fos gene expression in cardiac myocytes. *EMBO J* **15:**5535-5546.

Sharma C, Smith T, Li S, Schroepfer GJ Jr, and Needleman DH (2000) Inhibition of Ca^{2+} release channel (ryanodine receptor) activity by sphingolipid bases: mechanism of action. *Chem Phys Lipids* **104:**1-11.

Smith ER, Merrill AH, Obeid LM, and Hannun YA (2000). Effects of sphingosine and other sphingolipids on protein kinase C. *Methods Enzymol* **312:**361-373.

Spiegel S, and Milstien S (2003) Sphingosine-1-phosphate: an enigmatic signalling lipid. *Nat Rev Mol Cell Biol* **4:**397-407.

Titievsky A, Titievskaya I, Pasternack M, Kaila K, and Tornquist K (1998) Sphingosine inhibits voltage-operated calcium channels in GH4C1 cells. *J Biol Chem* **273:**242-247.

Voets T, Droogmans G, Wissenbach U, Janssens A, Flockerzi V, and Nilius B (2004) The principle of temperature-dependent gating in cold- and heat-sensitive TRP channels. *Nature* **430:**748-754.

Vriens J, Watanabe H, Janssens A, Droogmans G, Voets T, and Nilius B (2004) Cell swelling, heat, and chemical agonists use distinct pathways for the activation of the cation channel TRPV4. *Proc Natl Acad Sci U S A* **101:**396-401.

Watanabe H, Vriens J, Prenen J, Droogmans G, Voets T, and Nilius B (2003) Anandamide and arachidonic acid use epoxyeicosatrienoic acids to activate TRPV4 channels. *Nature* **424:**434-438.

Young KW and Nahorski SR (2002) Sphingosine 1-phosphate: a Ca^{2+} release mediator in the balance. *Cell Calcium* **32:**335-341.

Zager RA, Burkhart KM and Johnson A (2000) Sphingomyelinase and membrane sphingomyelin content: determinants of proximal tubule cell susceptibility to injury. *J Am Soc Nephrol* **11:**894-902.

Zygmunt PM, Petersson J, Andersson DA, Chuang H, Sorgard M, Di Marzo V, Julius D, and Hogestatt ED (1999) Vanilloid receptors on sensory nerves mediate the vasodilator action of anandamide. *Nature* **400:** 452-457.

Footnotes

The study was supported by the Deutsche Forschungsgemeinschaft, Fonds der Chemischen Industrie and Sonnenfeld-Stiftung.

C. G. and R. K. contributed equally to this study.

Molecular Pharmacology Fast Forward. Published on November 18, 2004 as DOI: 10.1124/mol.104.006734
This article has not been copyedited and formatted. The final version may differ from this version.

Figure legends

FIG. 1. TRPM3 is activated by D-erythro-sphingosine (SPH) in HEK293 cells. (A) Effect of 20 μM SPH on $[Ca^{2+}]_i$ in TRPM3-transfected cells. The black line indicates mean values from 8 independent experiments with at least 20 cells each. Gray areas depict the SEM for each data point. The dotted line represents mean values from 8 independent experiments with at least 20 non-transfected (NT) cells each. During application of SPH, 2 mM extracellular Ca^{2+} was exchanged for 2 mM EGTA. (B) Effect of 20 μM SPH on $[Ca^{2+}]_i$ in TRPM3-transfected cells in the presence of 2 mM EGTA and after addition of 2 mM extracellular Ca^{2+}. Shown are single cell traces from one representative fura-2 experiment out of 3 independent experiments with at least 20 cells each (mean value in black). (C) Mn^{2+} influx in TRPM3-transfected cells was enhanced by application of 20 μM SPH. Shown are mean values of 3 independent experiments with at least 15 cells each. The concentration of Mn^{2+} was 200 μM. (D) Concentration-response curve for the increase in $[Ca^{2+}]_i$ by SPH. Data points (mean ± SEM of n independent experiments with at least 20 cells each) were calculated from the SPH-induced responses 200 s after application of 1 μM (n = 4), 5 μM (n = 4), 10 μM (n = 13), 20 μM (n = 14) and 30 μM (n = 6). The concentration of SPH giving a half-maximal increase in $[Ca^{2+}]_i$ was 12 μM. (E) Stimulation of single TRPM3-transfected cells with hypotonic extracellular solution (200 mosmol/l) or with 20 μM SPH (in 300 mosmol/l) each increased $[Ca^{2+}]_i$. During application of SPH, 2 mM extracellular Ca^{2+} was exchanged for 2 mM EGTA. (F) Subsequent application of 20 μM SPH and hypotonic extracellular solution (200mosmol/l). Shown are traces of TRPM3-transfected cells from one representative fura-2 experiment out of 3 independent experiments with at least 20 cells each (mean value in black).

Molecular Pharmacology Fast Forward. Published on November 18, 2004 as DOI: 10.1124/mol.104.006734
This article has not been copyedited and formatted. The final version may differ from this version.

FIG. 2. Sphingosine is a specific stimulus for TRPM3. (A) Effects of 20 μM SPH on HEK293 cells transfected with diverse TRP channels C-terminally fused to enhanced green (eGFP) or yellow (YFP) fluorescent protein: hsTRPC3, mmTRPC4, mmTRPC5, hsTRPV4, mmTRPV5, mmTRPV6, hsTRPM2 and hsTRPM3. Bars represent the SPH-induced increases in $[Ca^{2+}]_i$ 200 s after application of SPH as means ± SEM of at least 3 independent fura-2 experiments with at least 20 cells each. (B) Effects of different fatty acids and lipids (AEA, AA, LNA, LA, OAG, DDG; 100 μM each) on TRPM3-transfected cells (filled bars) and non-transfected cells (open bars). Data were calculated from lipid-mediated increases in $[Ca^{2+}]_i$ 200 s after start of application, shown as means ± SEM of at least 3 independent fura-2 experiments each. *** $p < 0.001$, compared with non-transfected cells. (C) Shown are the chemical structures of the lipids DDG and SPH. (D) Effects of either DDG (100 μM) or SPH (20 μM) on HEK293 cells transfected with hsTRPC3. Shown are traces from representative fura-2 experiments with at least 15 cells each (mean value in black). (E) Effects of either DDG (100 μM) or SPH (20 μM) on HEK293 cells transfected with TRPM3. Shown are traces from representative experiments with at least 15 cells each (mean value in black).

FIG. 3. Activation of TRPM3-mediated currents by D-erythro-sphingosine (SPH) and by extracellular Ca^{2+}. (A) Whole-cell currents were continously recorded from a TRPM3-transfected cell at a holding potential of –60 mV. After application of 10 μM SPH, single-channel openings were resolved during a 1 s time interval. (B) Current-voltage relationship of SPH-induced single channel currents obtained from whole-cell recordings as shown in *(A)*. Each point represents mean values of single channel currents from independent experiments on one to three cells. (C) Currents were

Molecular Pharmacology Fast Forward. Published on November 18, 2004 as DOI: 10.1124/mol.104.006734
This article has not been copyedited and formatted. The final version may differ from this version.

recorded from a TRPM3-transfected and a non-transfected (NT) cell during voltage ramps from –100 mV to +100 mV (400 ms duration) at a holding potential of 0 mV. The insets above show the time courses of currents at –80 mV and +80 mV obtained from the voltage ramps. Extracellular Na^+-containing solution was substituted by either 100 mM $CaCl_2$ or 140 mM NMDG-Cl. Current–voltage relationships were obtained from responses before (a) and during (b) application of SPH and in the presence of 100 mM $CaCl_2$ and SPH (c). (D) Current–voltage relationships of SPH-induced currents obtained from recordings as shown in *(C)* were normalized to the cell capacitance. Data points represent mean current densities ± SEM from 10 cells in the presence of Na^+-containing solution (solid squares) and 100 mM $CaCl_2$ (open circles).

FIG. 4. Activation of TRPM3-mediated currents by depolarization. (A) 500 ms-voltage steps were applied from a holding potential of 0 mV to test potentials between –100 and +100 mV (increments of +20 mV). Corresponding whole-cell currents were recorded from a TRPM3-transfected cell during application of 10 µM SPH. The current-voltage relationship was constructed from the current amplitudes, obtained 450 ms after start of respective voltage-steps. (B) A 500 ms-prestep was followed by 500 ms-voltage steps between –100 and +100 mV (increments of +20 mV). Currents were recorded from a TRPM3-transfected cell during application of 10 µM SPH. Current-voltage relationships were constructed from the current amplitudes, obtained 1 ms (solid circles) and 450 ms (open squares) after start of respective voltage-steps. The dotted line represents a linear fit. (C) 500 ms-voltage presteps between –100 and +100 mV (increments of +20 mV) were followed by a 500 ms-voltage step to –100 mV. Currents were recorded from a TRPM3-transfected cell during application of 10 µM SPH. The fraction of open channels (F_{open}) was calculated by normalizing the

Molecular Pharmacology Fast Forward. Published on November 18, 2004 as DOI: 10.1124/mol.104.006734
This article has not been copyedited and formatted. The final version may differ from this version.

current amplitudes, obtained 1 ms after start of the step to -100 mV, to their maximal value. The dotted line represents a fit to a Boltzmann function of the form: $F_{open} = F_{const} + (1 – F_{const})/(1 + \exp((V – V_{1/2})/ s))$, where F_{open} represents the fraction of open channels at the prestep potential V, $V_{1/2}$ is the potential of half-maximal activation, s the slope paramater, and F_{const} the fraction of open channels at negative potentials. The fit yielded the following parameters: $F_{const} = 0.03$, $s = 27.9$ mV, $V_{1/2} = -61$ mV. (D) Currents were recorded from a TRPM3-transfected cell during voltage ramps from +100 mV to –100 mV (400 ms duration) following a 500 ms prepulse to +100 mV (see voltage protocol above). The holding potential was 0 mV. The inset shows the time course of currents at –80 mV obtained from the voltage ramps. Extracellular Na^+-containing solution was substituted by either 100 mM $CaCl_2$ or 140 mM NMDG-Cl. Current–voltage relationships were obtained from responses at corresponding time points (a, b).

FIG. 5. Stimulation of TRPM3 by D-erythro-sphingosine (SPH) is not mediated by store depletion, inositol 1,4,5-trisphosphate (IP_3) receptor activation or protein kinase C (PKC) inhibition. Effects of SPH application in non-transfected (NT) cells (A) and in TRPM3-transfected HEK293 cells (B) after pretreatment with thapsigargin (TG; 5 μM). Responses are shown as mean (black line) ± SEM (gray area) of one representative experiment from 5 similar experiments with at least 20 cells, each. (C) SPH-induced responses in TRPM3-transfected cells after treatment with the IP_3 receptor inhibitor xestospongin C (XS; 1 μM). During treatment with xestospongin C, no ATP- and CCh-induced Ca^{2+} responses were observed (100 μM each). Data are mean (black line) ± SEM (gray area) of one representative experiment out of 3 similar experiments with at least 20 cells each. (D) Shown are the effects of the protein

Molecular Pharmacology Fast Forward. Published on November 18, 2004 as DOI: 10.1124/mol.104.006734
This article has not been copyedited and formatted. The final version may differ from this version.

kinases inhibitor staurosporine (1 μM), the PKC inhibitor BIM I (1 μM) and SPH (20 μM) on TRPM3-transfected HEK293 cells as mean (black line) ± SEM (gray area) of one representative experiment out of 3 similar experiments with at least 20 cells each.

FIG. 6. Activation of TRPM3 by different sphingolipids. (A) Biosynthesis and degradation of sphingolipids (metabolizing enzymes shown in gray boxes; SPHK = sphingosine-kinase). (B) Effects of SPH (n = 8), DHS (n = 6) and DMS (n = 5) (20 μM each) on $[Ca^{2+}]_i$ in fura-2-loaded, TRPM3-transfected HEK293 cells. Traces represent means of n independent experiments with at least 20 cells, each. (C) Effects of diverse sphingolipids including the membrane permeable ceramides (C2- and C8-ceramide) on $[Ca^{2+}]_i$ in fura-2-loaded, TRPM3-transfected (filled bars) and non-transfected (open bars) cells. Data were calculated from sphingolipid-mediated responses 200 s after start of application, shown as means ± SEM of n independent experiments. * $p < 0.05$ and *** $p < 0.001$, compared with non-transfected cells. (D) Whole-cell currents were recorded during voltage ramps from +100 mV to –100 mV (400 ms duration) following a 500 ms-prepulse to +100 mV. The inset shows the time course of currents at –80 mV yielded from the voltage ramps. After obtaining the whole-cell configuration (arrow), the cell was perfused with a pipette solution containing 10 μM S1P. During application of 10 μM extracellular SPH, extracellular Na^+-containing solution was substituted by 100 mM $CaCl_2$. Current–voltage relationships were obtained from responses at corresponding time points (a, b).

Figure 1

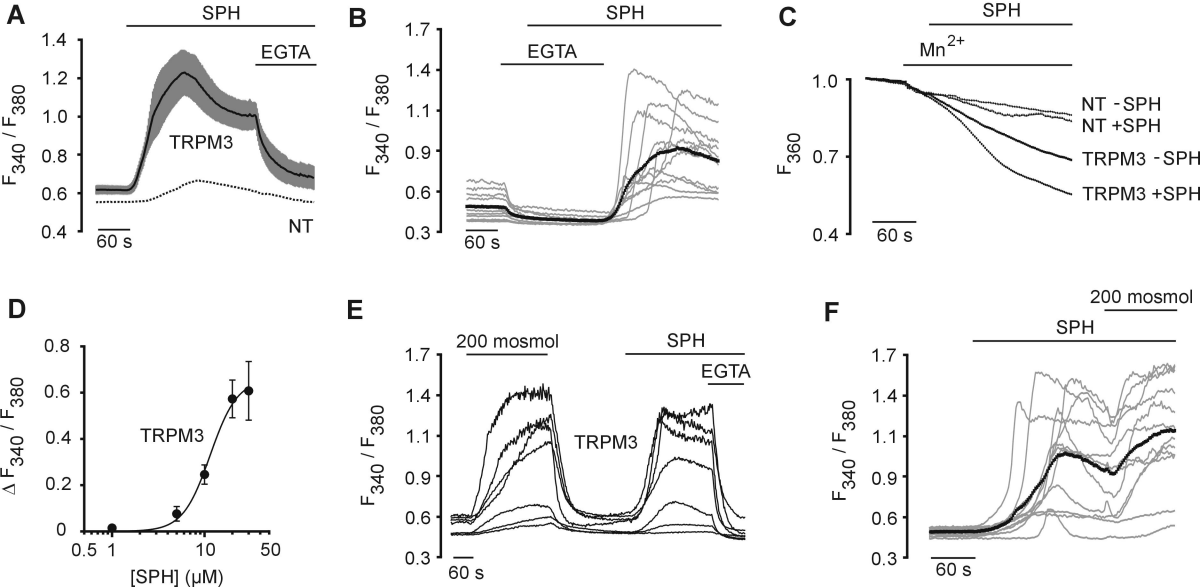
A
SPH
EGTA
TRPM3
NT
60 s
F340 / F380
B
SPH
EGTA
60 s
C
SPH
Mn2+
NT -SPH
NT +SPH
TRPM3 -SPH
TRPM3 +SPH
F360
D
TRPM3
ΔF340 / F380
[SPH] (μM)
E
200 mosmol
SPH
EGTA
TRPM3
F
200 mosmol
SPH

Figure 2

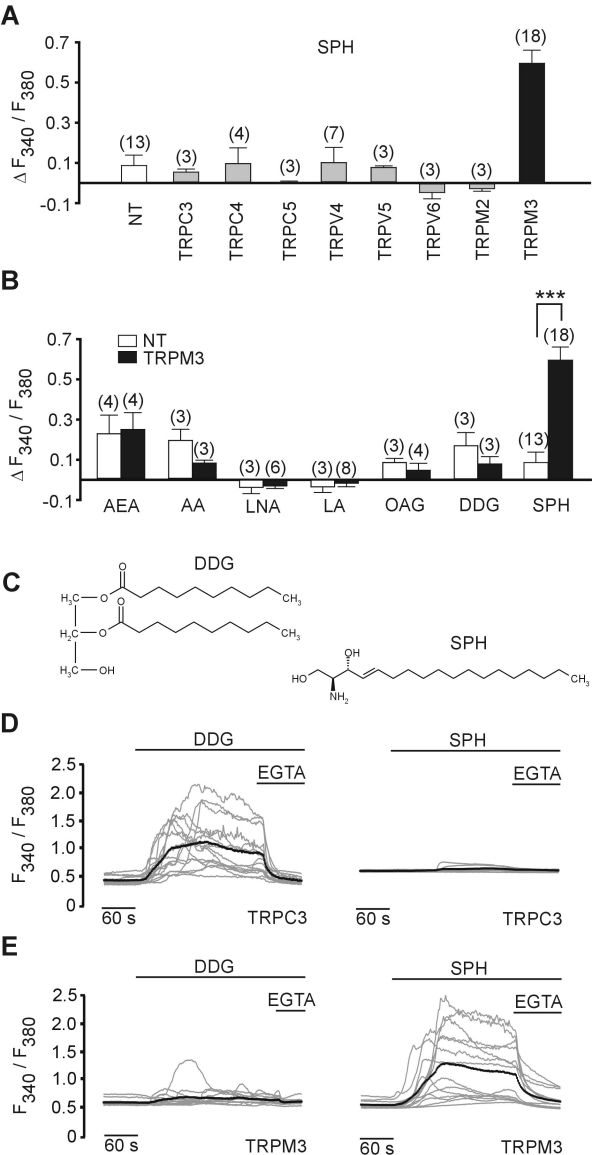
A
SPH
ΔF340 / F380
0.7
0.5
0.3
0.1
-0.1
(13)
(3)
(4)
(3)
(7)
(3)
(3)
(3)
(18)
NT
TRPC3
TRPC4
TRPC5
TRPV4
TRPV5
TRPV6
TRPM2
TRPM3
B
NT
TRPM3
***
(4) (4)
(3)
(3)
(3) (6)
(3) (8)
(3)
(4)
(3)
(13)
(18)
AEA
AA
LNA
LA
OAG
DDG
SPH
C
DDG
SPH
OH
HO
NH2
D
DDG
EGTA
SPH
EGTA
F340 / F380
2.5
2.0
1.5
1.0
0.5
0
60 s
TRPC3
E
DDG
EGTA
SPH
EGTA
TRPM3

Figure 3

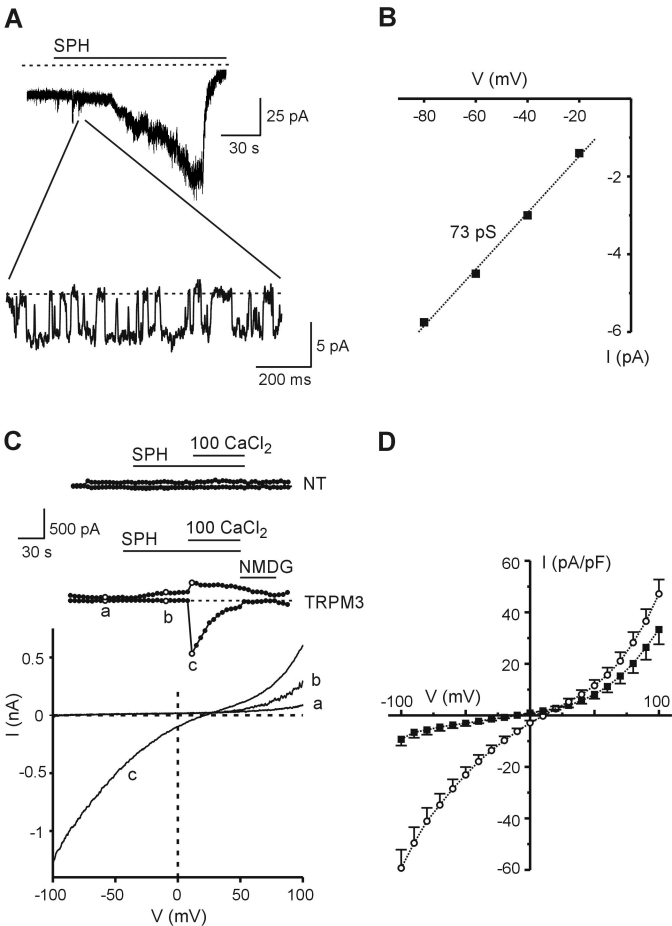
A
SPH
25 pA
30 s
5 pA
200 ms
B
V (mV)
-80
-60
-40
-20
-2
-4
-6
73 pS
I (pA)
C
SPH
100 CaCl2
NT
500 pA
30 s
SPH
100 CaCl2
NMDG
TRPM3
a
b
c
0.5
0
-0.5
-1
I (nA)
b
a
c
-100
-50
0
50
100
V (mV)
D
I (pA/pF)
60
40
20
-20
-40
-60
-100
V (mV)
100

Figure 4

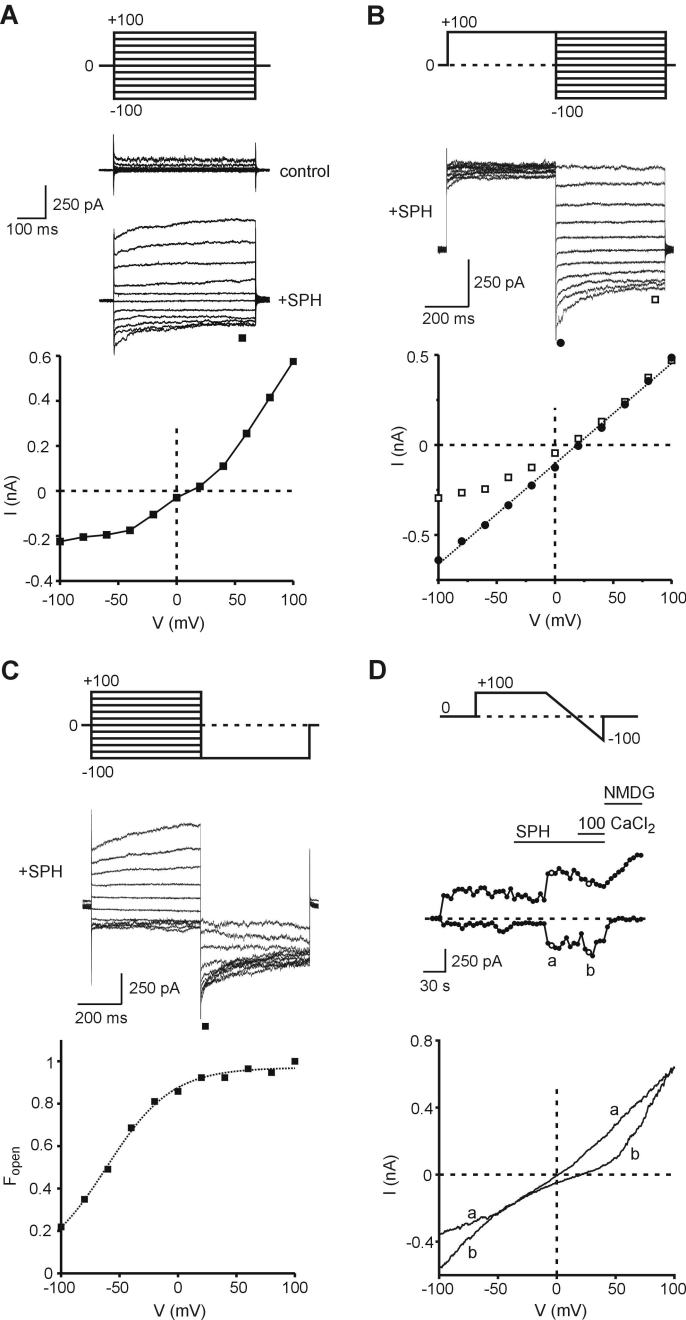
A
+100
0
-100
control
250 pA
100 ms
+SPH
0.6
0.4
0.2
0
-0.2
-0.4
I (nA)
-100
-50
0
50
100
V (mV)
B
+100
0
-100
+SPH
250 pA
200 ms
0.5
0
-0.5
I (nA)
-100
-50
0
50
100
V (mV)
C
+100
0
-100
+SPH
250 pA
200 ms
1
0.8
0.6
0.4
0.2
0
F open
-100
-50
0
50
100
V (mV)
D
+100
0
-100
NMDG
SPH
100 CaCl2
250 pA
30 s
a
b
0.8
0.4
0
-0.4
I (nA)
a
b
a
b
-100
-50
0
50
100
V (mV)

Figure 5

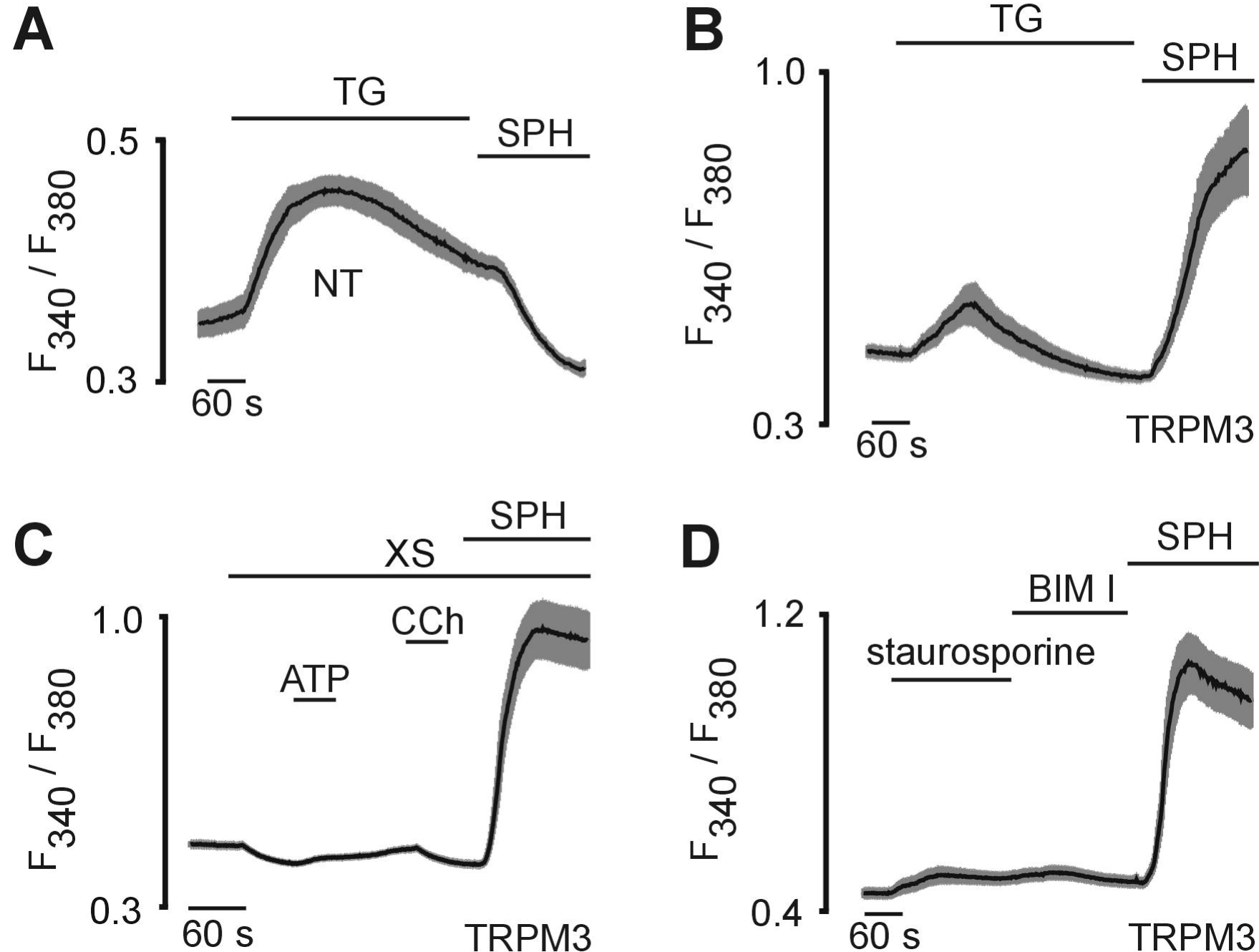
A
TG
SPH
0.5
0.3
F340 / F380
NT
60 s
B
TG
SPH
1.0
0.3
F340 / F380
60 s
TRPM3
C
SPH
XS
CCh
ATP
1.0
0.3
F340 / F380
60 s
TRPM3
D
SPH
BIM I
staurosporine
1.2
0.4
F340 / F380
60 s
TRPM3

Figure 6

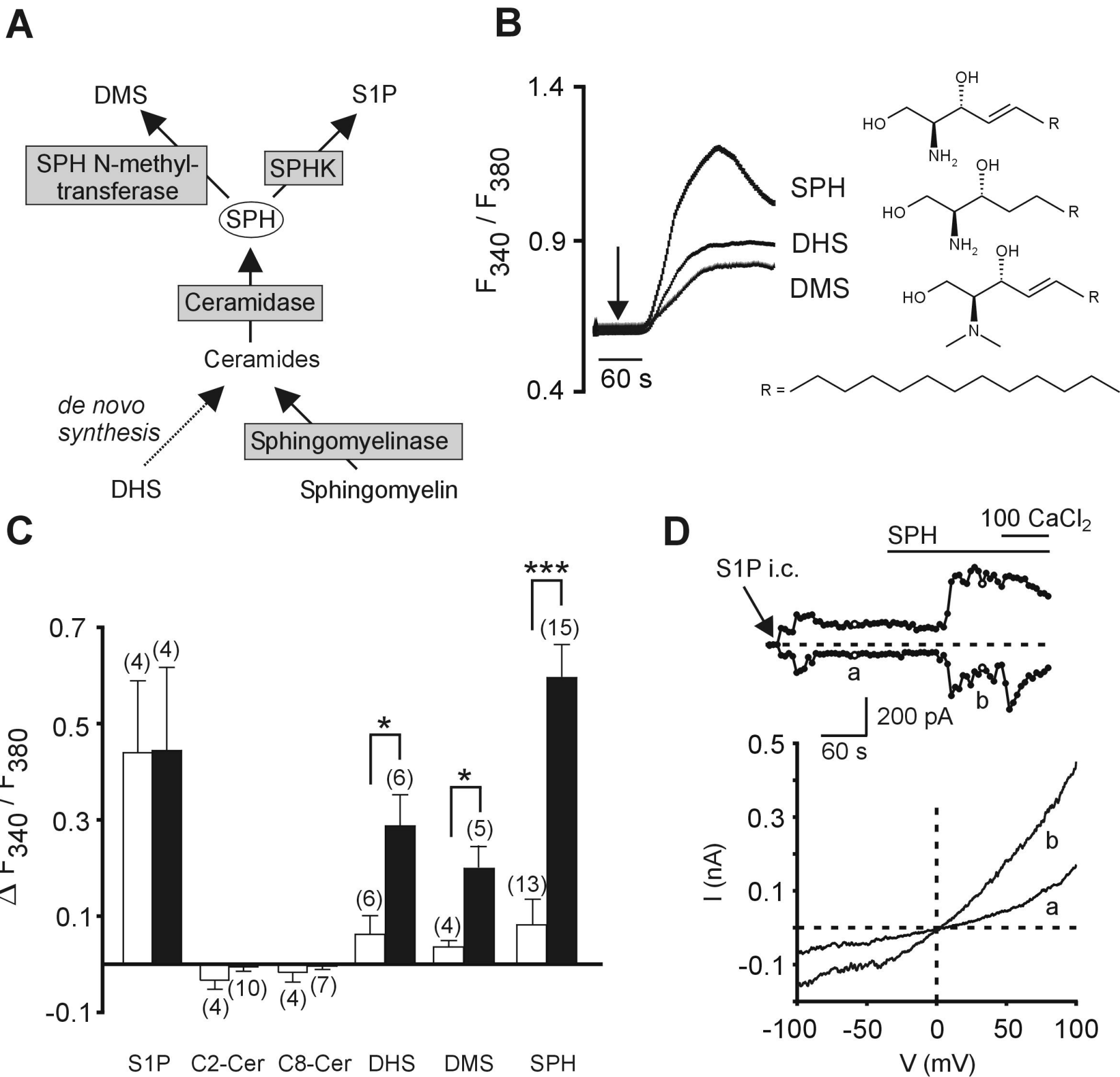
A
DMS
S1P
SPH N-methyl-transferase
SPHK
SPH
Ceramidase
Ceramides
de novo synthesis
Sphingomyelinase
DHS
Sphingomyelin
B
1.4
0.9
0.4
F340 / F380
60 s
SPH
DHS
DMS
HO
OH
NH2
R
N
R =
C
0.7
0.5
0.3
0.1
-0.1
Δ F340 / F380
(4)
(4)
(10)
(4)
(7)
(6)
(6)
(4)
(5)
(13)
(15)
*
*
***
S1P
C2-Cer
C8-Cer
DHS
DMS
SPH
D
100 CaCl2
SPH
S1P i.c.
a
b
200 pA
60 s
0.5
0.3
0.1
-0.1
I (nA)
-100
-50
0
50
100
V (mV)